New Intramolecular Fluorescence Probes That Monitor Photoinduced Radical and Cationic Cross-Linking

Bernd Strehmel,† John H. Malpert, Ananda M. Sarker, and Douglas C. Neckers*

Center for Photochemical Sciences,[1] Bowling Green State University, Bowling Green, Ohio 43403

Received May 18, 1999; Revised Manuscript Received September 9, 1999

ABSTRACT: The fluorescence probes *trans,trans*-1,4-bis[2-(2′,5′-dimethoxy)phenylethenyl)-2,3,5,6-tetrafluorobenzene (**1**) and *trans,trans*-1,4-bis[2-(3′,4′,5′-trimethoxy)phenylethenyl)-2,3,5,6-tetrafluorobenzene (**2**) show solvatochromic behavior yielding slopes in the Lippert−Mataga equation of −13 300 and −13 700 cm^{-1}, respectively. **1** sensitively probes progress in both photoinduced radical and cationic cross-linking. Both **1** and **2** show minor tendencies for *trans*−*cis* photoisomerization. Substituted stilbenes such as *trans*-2-(2′,5′-dimethoxyphenyl)ethenyl-2,3,4,5,6-pentafluorobenzene (**1r**) and *trans*-2-(3′,4′,5′-trimethoxyphenyl)ethenyl-2,3,4,5,6-pentafluorobenzene (**2r**) are less solvatochromic in fluorescence but evidence enhanced tendency toward photoisomerization.

Introduction

Fluorescence cure monitoring has become an important tool in material science and engineering.[2−7] Though other techniques such as NMR[8] and ESR spectroscopy[9] provide useful structural information, fluorescence techniques offer the opportunity for on-line applications. They provide an alternative to real time FTIR spectroscopy,[10] as well as information about both the progress of polymer formation and the molecular mobility of a probe in the material investigated. The probe approaches optimal performance if, under chosen experimental conditions, the intrinsic or inherent fluorescence of the material being polymerized is negligible and the signal seen in emission can be assigned to the probe exclusively.

Though various reports have suggested the inherent fluorescence of a polymer/monomer system can be used to monitor cure, this fluorescence generally bears little relationship to matrix parameters.[5,11] The nature of the emitting species cannot be accurately characterized since even impurities (i.e., traces of catalysts or byproducts) may fluoresce. Thus, most practitioners employing fluorescence emission as a monitor for cure prefer to add an external probe in small amounts to the reaction mixture.

For example, an intrinsic fluorescence was reported as tracking the polymerization of bisphenol A−diglycidyl ether and 4,4′-diaminodiphenyl sulfone[12] and suggested this to be medium dependent.[13] Cross-linking changes the mobility of the self-contained fluorophore, resulting in significant changes in the spectra as a function of the excitation wavelength.Compounds that show a fluorescence that is influenced by either the viscosity or the dipolar relaxation of the matrix are favored for monitoring changes in molecular environment. Nevertheless, careful consideration necessitates the interpretation of the results due to reabsorption. Among the compounds used for this recently have been 4-(dimethylamino)-4′-nitrostilbene,[2a] coumarins,[2a] (dimethylamino)-naphthalenesulfonamides,[2b−d] and 1-phenyl-4-(4-cyano-1-naphthylmethylene)piperidine.[14] 4-(Dimethylamino)-4′-nitrostilbene and 1-phenyl-4-(4-cyano-1-naphthylmethylene)piperidine show the largest spectral changes with changes in solvent polarity, but low emission quantum yields in polar materials occasionally restrict the application of these compounds. Many molecules may form additional species in the excited state accompanied by changes in molecular geometry. Furthermore, species formed in the excited state may deactivate either with or without radiation. Such alternative excited-state deactivation reactions result in a decrease in fluorescence quantum yield (Φ_f) as well as a reduction fluorescence decay time (τ_f).[15] They may also lead to additional emission.

We thus divide probes into two main groups: (i) compounds forming a nonradiative species in the excited state (group A) and (ii) compounds forming a radiative species (group B). Typical group A probes include compounds showing efficient formation of either intramolecular charge transfer (ICT)[3a,4b,c,16,17] or probes that undergo trans−cis isomerization.[18,19] Because the energy gap between the excited state and ground state is small in either the ICT or the perpendicular twisted state in the case of compounds that undergo isomerization, deactivation occurs mainly without radiation. *N*,*N*-Dialkylbenzylidenemalodinitriles are group A probes pioneered in the early 1980s for monitoring thermal polymerization of methacrylates.[3] The formation of ICT reliably influences changes in the fluorescence quantum yield. Furthermore, both ICT probes and trans−cis probes that undergo isomerization can be used to examine the cross-linking of epoxy−amine systems by measurements of the decay time τ_f using time-correlated single photon counting.[4]

Group B probes include excimers (group B1)[7a,20] as well as dual-emitting ICT probes (group B2).[2,7c,21] The dual emission of excimers depends only on the molecular mobility (relaxation of free volume),[20] while the dual emission of ICT probes can be influenced by both the molecular mobility and the matrix polarity.[2,7] Excimer formation correlates directly with the α-relaxation of a material.[20] Such probes show no intramolecular excimer formation in glassy materials because the reaction volume necessary is too large. Group B2 probes have received the most recent attention since they may sense changes in a material by either a change of the spectral

† Present address: University of Applied Sciences Merseburg, D-06217 Merseburg, Germany.

10.1021/ma990773b CCC: $18.00
Published on Web 10/15/1999

shape (ratio method)[2b,c] or registration of the emission maximum for ICT species (maximum method).[2a]

Most of the common ICT probes contain amino groups that are often reactive in the matrix being polymerized. Since polyenes bear no nucleophilic groups, we thought they might provide an alternative. In these compounds, isomerization of the double bond yielding stable cis isomers is the main side reaction competing with fluorescence. Although fluorescence of the cis isomers also occurs,[22] deactivation often also occurs without radiation.[19]

The goal of this work was to develop a probe showing a strong medium-dependent fluorescence and relatively high fluorescence quantum yields in polar solvents (>40%). A red shift of the probe was also preferred in order to avoid interference by the strong self-fluorescence of the cured epoxides. A high molar absorption coefficient is also preferred so as to maintain low probe concentrations. Given this, we anticipated a probe that would be useful in monitoring both photoinduced radical and cationic cross-linking reactions.

The probes introduced in this publication show strong medium-dependent fluorescence with a change in solvent polarity, they are highly fluorescent, and they also possess good absorption characteristics. Certain photophysical details were previously reported.[21]

Experimental Part

Synthesis of the Materials. (a) General Information. All manipulations were performed under argon. Reagents and solvents were purchased from Aldrich and used without further purification. NMR spectra were taken with a Varian Gemini 200 NMR spectrometer. GC/MS were measured on a Hewlett-Packard 5988 mass spectrometer coupled to an HP 5880A GC with a 30 m × 0.25 mm i.d. × 0.25 mm film thickness DB-5 ms column (J & B Scientific), interfaced to an HP 2623A data processor. UV−vis spectra were obtained using a HP 8452 diode array spectrophotometer. Molar absorption coefficients were measured in toluene. Infrared spectroscopy was performed using a Mattson Instruments 6020 Galaxy series FT-IR spectrometer. High-resolution mass spectra were obtained from the Mass Spectrometry Laboratory in the University of Illinois at Urbana-Champaign. Thin-layer chromatography was performed on Sigma-Aldrich plates (layer thickness 250 μm, particle size 5−17 μm, pore size 60 Å) purchased from Aldrich. Silica gel chromatography was performed using silica gel (40 μm, 32−63 μ) purchased from Scientific Adsorbents Inc. Melting points were determined using a capillary melting point apparatus (Uni-melt, Arthur H. Thomas Co., Philadelphia, PA).

Reichardt's dye (2,6-diphenyl-4-(2,4,6-triphenylpyridinio)-phenolate) was purchased from Aldrich and used without any additional purification. The photoinitiator 2,2′-dimethoxy-2-phenylacetophenone (Ciba Specialty Chemicals) was purified by recrystallization from hexanes. The synthesis of *trans,trans*-1,4-bis[2-(2′,5′-dimethoxy)phenylethenyl)-2,3,5,6-tetrafluorobenzene (**1**) was previously reported.[21]

(b) *trans,trans*-1,4-Bis-[2-(3′,4′,5′-trimethoxy)phenylethenyl)-2,3,5,6-tetrafluorobenzene (2). To a cooled solution (0 °C) of NaH (6 equiv, prewashed with hexanes) in THF (1 M) was added dropwise via cannula a solution of the tetramethyl 2,3,5,6-tetrafluoro-*p*-xylyldiphosphonate (1 equiv) in THF (0.15 M). The mixture was allowed to stir for 30 min, and then a solution of 2,5-dimethoxybenzaldehyde (2.05 equiv) in THF (0.5 M) was added via cannula. The reaction was monitored by TLC until completion. The solution was carefully quenched with water and extracted with ether. In some cases the product crystallized from the ether solution, and the crystals were filtered and collected. The organic layer was dried over $MgSO_4$ and concentrated. The final compound was filtered from the organic layer and recrystallized from benzene

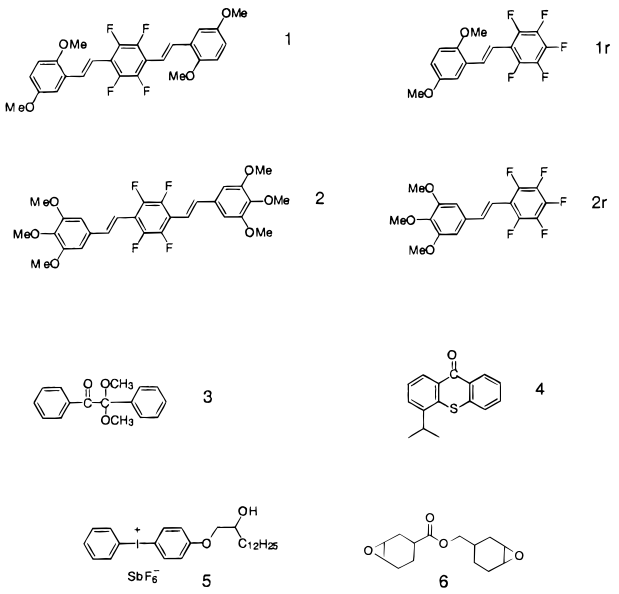

to provide yellow crystals in 97% yield. ^{1}H NMR ($CDCl_3$): δ 7.45 (d, J = 16.8 Hz, 1H), 6.98 (d, J = 16.8 Hz, 1H), 6.77 (s, 2H), 3.94 (s, 6H), 3.89 (s, 3H). IR (neat): 965, 1130, 1583. MS (EI): 534, 267. HRMS (M^+) calculated for $C_{28}H_{26}F_4O_6$: 534.1666; found 534.1650. mp = 213−215 °C; lg ϵ_{max}(toluene) = 4.78 (in M^{-1} cm^{-1}).

(c) Dimethyl 2,3,4,5,6-Pentafluorobenzylphosphonate. 2,3,4,5,6-Pentafluorobenzyl bromide (2.49 g, 9.92 mmol) was dissolved in trimethyl phosphite (4.0 mL) solution and heated at 90 °C for 2 days, and the solvent distilled off under reduced vacuum. The remaining material was taken up in hexanes and washed with water. The compound was used without further purification. ^{1}H NMR ($CDCl_3$): δ 3.77 (d, J = 11.0 Hz, 3H), 3.23 (d, J = 22.0 Hz, 1H).

(d) *trans*-2-(2′,5′-Dimethoxyphenyl)ethenyl-2,3,4,5,6-pentafluorobenzene (1r). A solution of 2,5-dimethoxybenzaldehyde (0.530 g, 3.19 mmol) and the corresponding aryl phosphonate (0.926 g, 3.19 mmol) in THF (5 mL) was added via cannula to a solution of NaH (0.459 g, 19.1 mmol, prewashed with hexanes) in THF (5 mL) at 0 °C. The solution was stirred overnight, carefully quenched with water, and extracted with ether. The solution was concentrated and passed through a short column of silica gel. The resultant crystals were then recrystallized in EtOH to give 0.744 g (71% yield) of a white crystalline solid. ^{1}H NMR ($CDCl_3$): δ 7.74 (d, J = 17.2 Hz, 1H), 7.11 (bs, 1H), 6.98 (d, J = 17.2 Hz, 1H), 6.87 (s, 1H), 6.83 (s, 1H), 3.85 (s, 3H) 3.83 (s, 3H). IR (neat): 811, 976, 1048, 1505, 2840. TLC (hexanes/ethyl acetate 5:1): R_f = 0.57. MS (EI): 330, 315, 181. HRMS (M^+) calculated for $C_{16}H_{11}F_5O_2$: 330.0679; found 330.0683. mp = 92−94 °C; lg ϵ_{max}-(toluene) = 4.03 (in M^{-1} cm^{-1}).

(e) *trans*-2-(3′,4′,5′-Trimethoxyphenyl)ethenyl-2,3,4,5,6-pentafluorobenzene (2r). A solution of 3,4,5-trimethoxybenzaldehyde (1.14 g, 5.80 mmol) and the corresponding phosphonate (1.73 g, 5.96 mmol) in THF (15 mL) was added via cannula to a solution of NaH (0.572 g, 23.8 mmol, prewashed with hexanes) in THF (10 mL) at 0 °C. The solution was stirred overnight, carefully quenched with water, and extracted with ether. The solution was concentrated and passed through a short column of silica gel. The resultant crystals were then recrystallized twice in EtOH to give 1.17 g (56% yield) of a white crystalline solid. ^{1}H NMR ($CDCl_3$): δ 7.35 (d, J = 16.8 Hz, 1H), 6.86 (d, J = 16.6 Hz, 1H), 6.74 (s, 2H), 3.93 (s, 6H) 3.88 (s, 3H). IR (neat): 809, 994, 1131, 1496, 2842. TLC (hexanes/ethyl acetate 10:1): R_f = 0.25. MS (EI): 360, 231, 181. HRMS (M^+) calculated for $C_{17}H_{13}F_5O_3$: 360.0785; found 360.0786. mp = 124−127 °C; lg ϵ_{max}(toluene) = 4.35 (in M^{-1} cm^{-1}).

Methods. (a) Stationary Fluorescence. Fluorescence spectra were recorded with a Spex Fluorolog 2 equipped with

Table 1. Absorption Maximum (λ_{max}^{abs}), Fluorescence Maximum (λ_{max}^{flu}), and Fluorescence Quantum Yield (Φ_f) for the Compounds 1, 2, 1r, and 2r Obtained in Different Solvents

compd	solvent	λ_{max}^{abs} (nm)	λ_{max}^{flu} (nm)	Φ_f
1	toluene	386	441	0.91
	THF	384	476	0.84
	CH_3CN	380	510	0.72
2	toluene	378	448	0.62
	THF	370	478	0.58
	CH_3CN	362	507	0.46
1r	toluene	352	422	0.52
	THF	352	443	0.51
	CH_3CN	348	457	0.44
2r	toluene	326	417	0.04
	THF	322	441	0.04
	CH_3CN	318	431	0.05

both excitation and emission double-beam monochromators. All spectra were corrected (band-pass 2.8 nm) and were measured in perpendicular geometry using 1 cm quartz cuvettes. Fluorescence quantum yields are relative to 9,10-diphenylanthracene in cyclohexane as external standard (Φ_f = 0.9 in cyclohexane[23]). All solutions were air-saturated.

(b) Cure Monitoring. The cure monitor setup has been described previously.[2c] All cross-linking reactions were carried out between two glass plates having a thickness of 175 μm. The concentration of the probe was adjusted to be 0.01 wt % in the monomer. The concentration of the radical photoinitiator 2,2′-dimethoxy-2-phenylacetophenone (Ciba Specialty Chemicals) was 10^{-2} M. Cationic cross-linking required the use of a hybrid photoinitaitor system containing 1 wt % 7-isopropylthioxanthone (Great Lakes Chemical) and 2.5 wt % (4-(2′-hydroxytetradecyloxy)phenyl)phenyliodonium hexafluoroantimonate (Sartomer), which were dissolved in the monomer mixture consisting of 80 wt % 3,4-epoxycyclohexylmethyl 3,4-epoxycyclohexylcarboxylate and 20% glycerol (Union Carbide). Polychromatic light from a 150 W xenon lamp (from Xenon Corp.) was used in order to illuminate the cross-linking material offline. Calibration against FTIR (Galaxy) was done separately. For this purpose, the reaction mixture was placed between two KBr plates (thickness was adjusted by using of appropriate spacers) and irradiated with the same light source. Both data for IR spectra and cure monitor ratios were measured at different irradiation times and compiled to get a set of reliable data describing the dependence between fluorescence cure monitor data and conversion over a reasonable range. Double-bond conversion was measured for the disappearance of the absorption at 810 cm^{-1}. The data were correlated with the ratio of the fluorescence intensities obtained at 433 and 520 nm by the cure monitor.

Results and Discussion

Photophysical Properties in Ordinary Solvents. Recently, we reported the dependence of the fluorescence of **1** on the polarity of the solvent.[21] Both substitution of alkoxy functions on the terminal aromatic rings and perfluoro substitution were responsible for tuning the fluorescence as a function of matrix polarity. In this work, we also include compound **2** that bears different alkoxy substituents on the terminal aromatic rings. Differences in substitution may affect photophysical behavior because the electron density of the aromatic system differs. The photophysical data (absorption maximum λ_{max}^{abs}, fluorescence maximum λ_{max}^{flu}, fluorescence quantum yield Φ_f) reported in Table 1 show that changes resulting from changes in the molecular surrounding are similar for **1** as well as **2**.

Matrix-dependent fluorescence can be described by a two-state reaction mechanism[15] wherein the emission is a sum of both the locally excited state (LE) and the matrix-sensitive emitting species. The latter is likely a charge transfer state (CT),[21] since the emission of LE does not significantly differ upon changing solvent polarity, but the CT emission is tunable as a result of matrix polarity. The fluorescence spectra for **1** and **2** in common solvents are shown in Figure 1. Scheme 1 shows a possible mechanism describing the relationship between solvent-dipole orientation, reorganization after excitation, and possible molecular orbital patterns that can be involved in the electronic excitation of the CT.[24] Luminescence quantum yields obtained for **1** and **2** (Table 1) are remarkably high despite strong competition between deactivation of the LE and formation of the CT. The CT possesses highly allowed transitions from the excited state into vibrational levels of the ground state.[21]

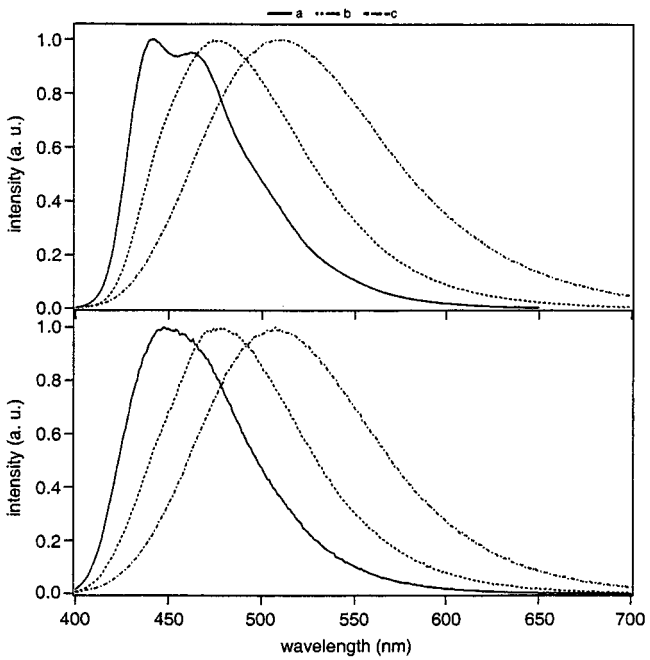

Figure 1. Fluorescence spectra of **1** and **2** in several solvents (a, toluene; b, tetrahydrofuran; c, acetonitrile).

Scheme 1. Schematic Description for the Reorientation of Dipolar Matrix Molecules around a Probe Showing Classical Charge Transfer

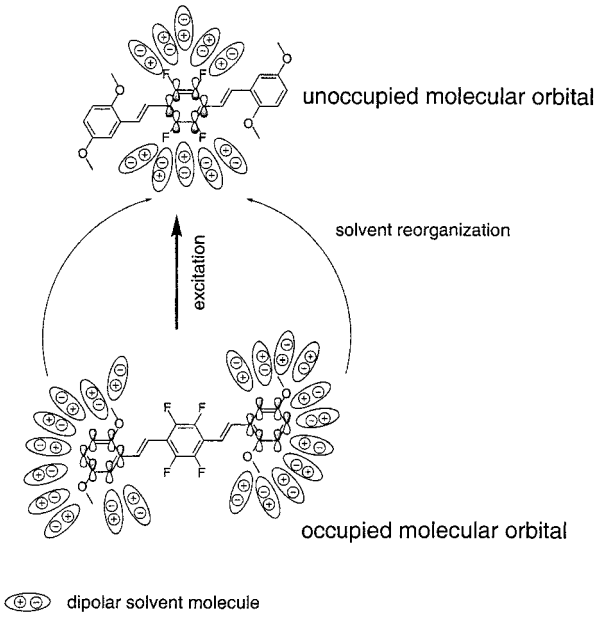

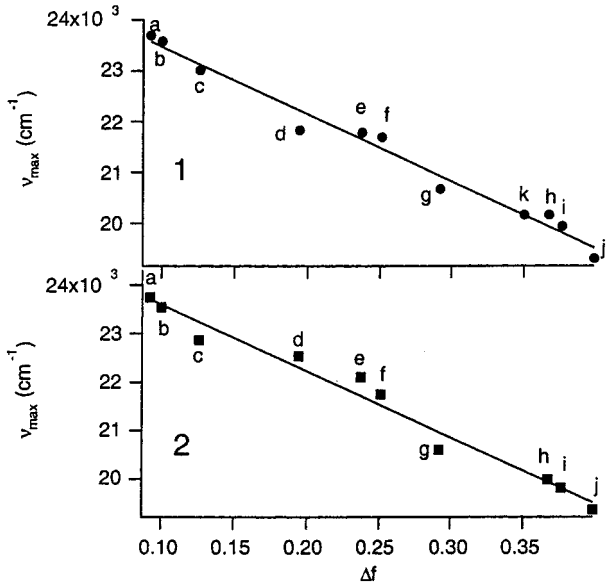

Figure 2. Lippert−Mataga plot (eq 1) for **1** (top) and **2** (bottom) (solvents: a = hexane, b = cyclohexane, c = toluene, d= dibutyl ether, ae = diisopropyl ether, f = diethyl ether, g = tetrahydrofuran, h = butanone, i = butyronitrile, j = acetonitrile, k = TEGDA).

Table 2. Results Obtained for the Solvatochromic Slope According to Eq 1 with the Corresponding Correlation Coefficient *r*

compound	slope (cm^{-1})	*r*
1	−13300	0.990
2	−13700	0.988
1r	−7100	0.990
2r	−6600	0.998

Though originally developed for dipolar molecules, eq 1[25] can be used to evaluate probe sensitivity because one can obtain a quantity describing the response to solvent polarity changes from its slope. Though neither **1** nor **2** possesses a dipole moment due to symmetry restrictions, one can use eq 1 to compare the sensitivity of the new compounds as probes with literature data.[25] The spectral shift of fluorescence according to eq 1 can be explained by the reorganization of partial charges in the molecular orbitals involved according to Scheme 1.

$$\nu_{CT} = \text{const} - \frac{1}{4\pi hc\epsilon_0}\frac{2}{\rho^3}\mu_{CT}^{exc}(\mu_{CT}^{exc} - \mu_{CT}^{GS(FC)})\Delta f = \text{const} + \text{slope} \times \Delta f \quad (1)$$

(ν_{CT} = emission energy in the corresponding solvent, ϵ_0 = permittivity in a vacuum, Δf = solvent polarity parameter,[25] ρ = Onsager radius,[25] h = Planck's constant, μ_{CT}^{exc} = dipole moment of the CT in the excited state, $\mu_{CT}^{GS(FC)}$ = dipole moment of the CT in the ground state with Franck−Condon geometry).

When plotted using eq 1, both **1** and **2** result in a straight line (Figure 2). Solvatochromic sensitivity is similar in both despite different substitution patterns on the terminal aromatic rings (Table 2). Further, the slopes each sufficiently probes a change of solvent polarity in organic materials. However, highly solvatochromic materials slopes can be as high as >25 000 cm^{-1},[2a,b,d,7c,14] but the absolute values (Φ_f) are small in comparison. Neither **1** nor **2** undergoes significant trans−cis photoisomerization in solvents of medium

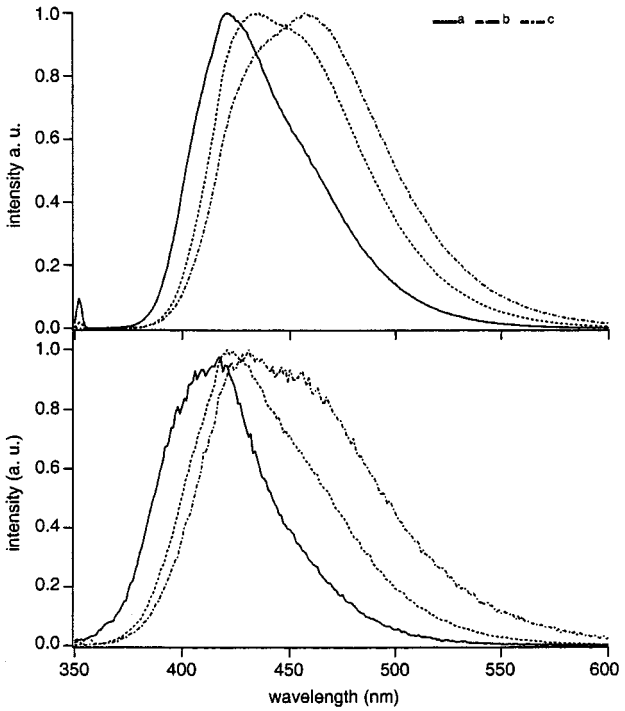

Figure 3. Fluorescence spectra for **1r** and **2r** (a, toluene; b, tetrahydrofuran; c, acetonitrile).

polarity, and relatively high emission yields, even in polar solvents, suggest each should be quite sensitive. Since the observed emission may result from at least two isomers in either **1r** or **2r**, both of which may effect the overall fluoresence,[26] the resulting emission signal is not easily treated.

The solvent polarity parameter Δf [25] for tetraethylene glycol diacrylate (TEGDA) was obtained using Reichart's dye.[27] In the monomer it showed an absorption maximum of 656 nm corresponding to an E_T[30] value[27] of about 182.2 kJ/mol. Comparison with several solvents (Figure 2) yielded a Δf value for TEGDA of ≈0.35, confirming the monomer to be quite polar. Solvent relaxation times increase with prolonged photoinduced cross-linking and result in a poorer solvation of CT (Scheme 1), and this shifts the emission to the blue. No significant changes in emission spectra are expected in the case of nonpolar cross-linkable systems because little change in polarity occurs in such systems as a result of photoreaction.

It is uncertain whether substitution of the fluorinated ring at the 1,4-position with two adjacent styryl groups is necessary to obtain a probe with a reasonable solvatochromic behavior and high fluorescence quantum yield or if only one styryl group is sufficient to probe the molecular surroundings. Reference compounds **1r** and **2r**, which bear only one adjacent styryl group, were synthesized to address this. These compounds can be thought of as donor−acceptor compounds possessing a specific dipole moment in the ground state. Though the fluorescence spectra obtained show a change in shape and position (Figure 3), the changes observed are smaller than for either **1** or **2**. The spectra show two emissions, depending on solvent, that are generally assigned to two species. But the overlap of both emissions from the LE and CT complicates locating the fluorescence maximum for the CT, which is necessary in order to evaluate solvatochromic sensitivity according to eq 1.

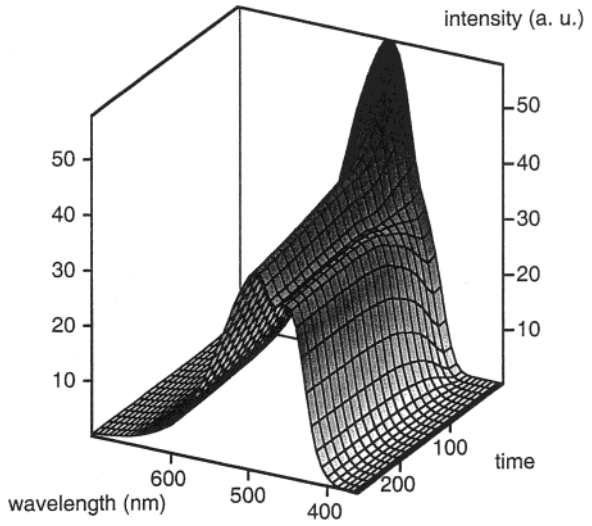

Figure 4. Change of the fluorescence spectra of **1** during photoinduced radical polymerization in TEGDA as a function of reaction time (λ_{exc} = 350 nm).

Compounds **1r** and **2r**, because the conjugated system is smaller, show the expected hypsochromic shift in absorption when compared to either **1** or **2** (Table 1). **2r** also shows a lower fluorescence quantum yield likely caused by a stronger contribution of nonradiative deactivation processes, e.g., trans−cis photoisomerization.[28]

Model compounds **1r** and **2r** absorb mainly in the UV. Since these compounds show smaller spectral changes with a change in matrix polarity than either **1** or **2**, they are not sufficiently sensitive to be used as probes for cure monitoring. Furthermore, trans−cis photoisomerization changes the absorption profile during cross-linking because a photostationary state is formed during reaction. Thus, a constant absorption is not fulfilled for compounds **1r** and **2r**. The compounds also show enhanced photochemistry so they will not be considered further in this work.

Perfluoro substitution on the central aryl group and substitution of the terminal rings at either the 2,5- or 3,4,5-position with alkoxy groups yields reasonable fluorescent probes for monitoring the photoinduced cross-linking process of vinyl and oxiranyl monomers. Both **1** and **2** show relatively high fluorescence quantum yields and significant changes in spectral profile with a change in the molecular surroundings. Because both **1** and **2** possess similar solvatochromic emission properties, we emphasize the probe behavior of **1** during photoinduced radical and cationic cross-linking.

Cure Monitor Profiles in Radical Polymerization. The typical cure monitor profile for **1** in TEGDA using 2,2′-dimethoxy-2-phenylacetophenone (**3**) as the photoinitiator (Figure 4) clearly shows the growth of a new band in the blue region while the emission in the red region decreases with prolonged photoinduced cross-linking of the monomer. This result supports that two excited states are responsible for spectral changes in the probe in this monomer, the polymerization of which proceeds to relatively high conversion. Decrease in molecular mobility increases the matrix dipole relaxation time and results in a poorer stabilization of the CT (Scheme 1). Thus, the energy of the CT increases and results in a blue shift of the spectra. The LE gains emission intensity because the rate of CT formation ($k_{LE \rightarrow CT}$) drops with decreasing molecular mobility.[29]

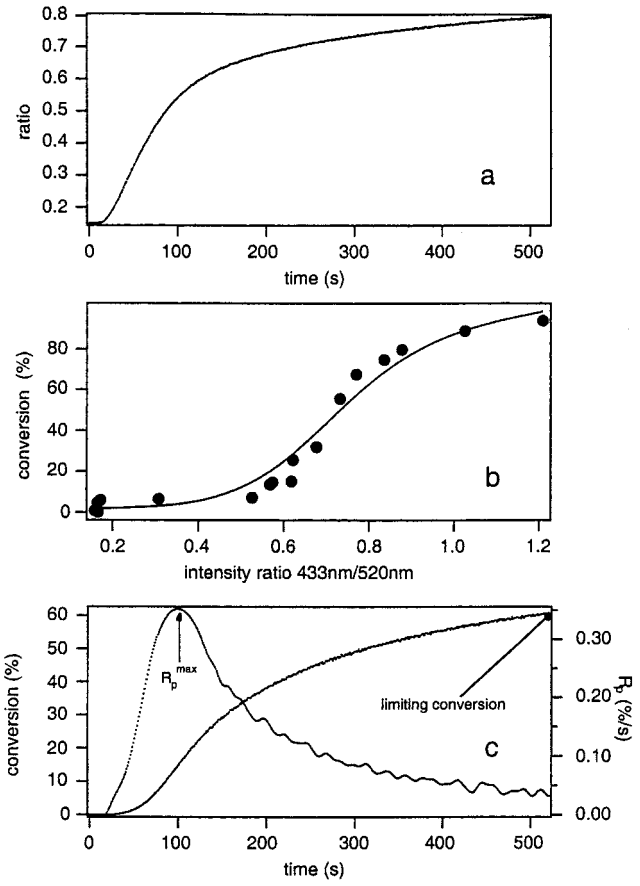

Figure 5. Cure monitor data obtained for radical cross-linking of TEGDA for the probe **1** (a) as a function of reaction time for the fluorescence intensity, (b) as a function of conversion on double bonds for the corresponding intensity ratio 433 nm/520 nm, and (c) for both double-bond conversion and polymerization rate R_p after transformation of the data.

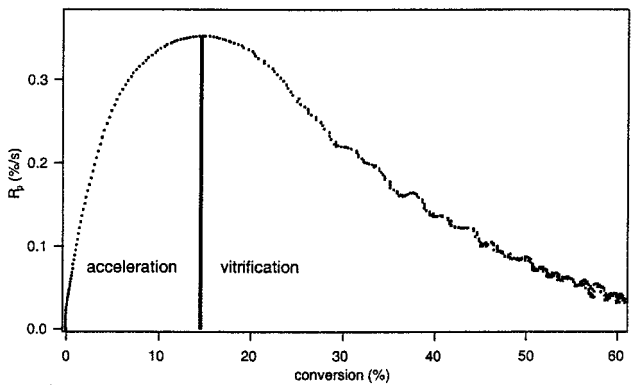

Figure 6. Construction of the polymerization rate (in %/s) as a function of double-bond conversion by using the data obtained from Figure 5.

The most significant changes in the spectra occur at 433 nm (λ_1) and 520 nm (λ_2). A plot of the ratio of the intensities at these two wavelengths, $I(\lambda_1/\lambda_2)$ (Figure 5a) reports changes in molecular surrounding of the probe in the cross-linking matrix and can be related to the free volume model. Calibration of the data against conversion, i.e., FTIR, yields a calibration function (Figure 5b) that depends on the nature of the monomer and the detection system used.[30] This treatment allows construction of a profile for conversion from fluorescence cure monitor data (Figure 5c).

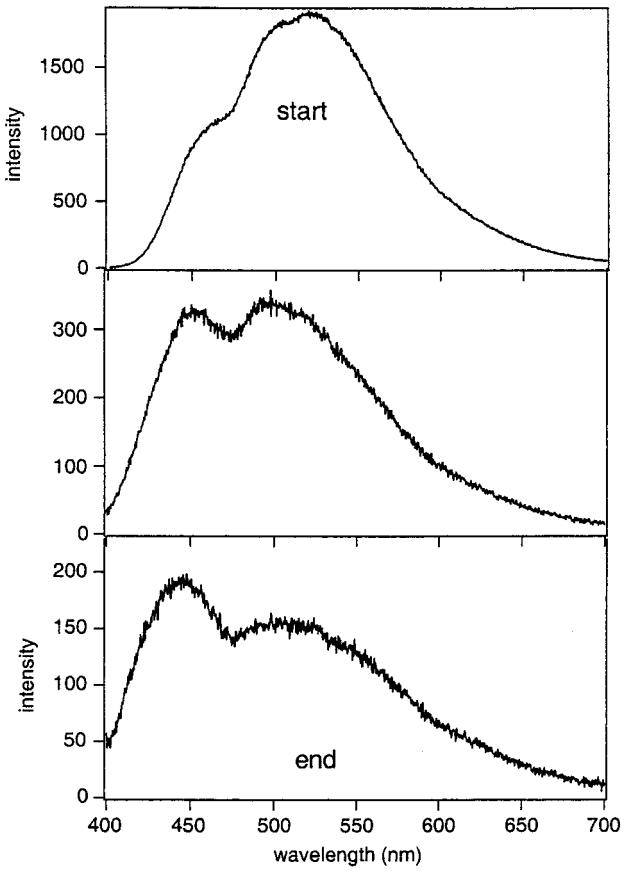

Figure 7. Fluorescence spectra of **1** obtained at different irradiation time during cationic cross-linking (top, $t = 0$; middle, $t = 30$ s; bottom, $t = 60$ s).

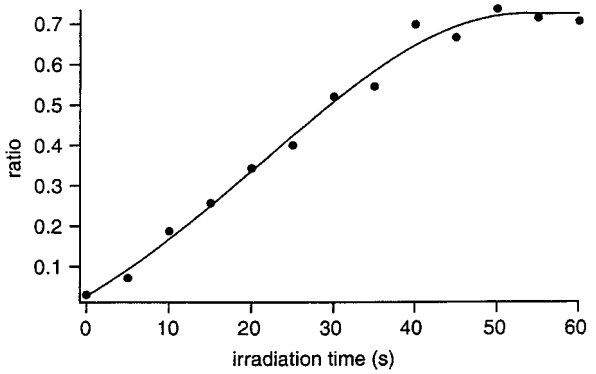

Figure 8. Plot of the fluorescence ratio (433 nm/520 nm) of **1** obtained at different irradiation times during cationic cross-linking.

A plot of dx/dt vs conversion closely resembles the reaction profile during cross-linking and clearly demonstrates acceleration until the maximum of the polymerization rate (R_p^{max}) is reached and vitrification of the system after passing the point R_p^{max}.[14,85] One example showing the dependence of dx/dt as a function of conversion is given in Figure 6.

Cure Monitor Profiles in Cationic Cross-Linking. A hybrid photoinitiator system consisting of 7-isopropylthioxanthone (**4**) and (4-(2′-hydroxytetradecyloxy)-phenyl)phenyliodonium hexafluoroantimonate (**5**) was chosen for efficient photoinduced polymerization of epoxy resin. 3,4-Epoxycyclohexylmethyl 3,4-epoxycyclohexylcarboxylate (**6**) containing 20 wt % glycerol was used as the monomer.

Spectral changes of **1** are similar to those for the radical cross-linking system occurring during cationic cross-linking of **6** (Figure 7). A plot of the intensity ratio 430 nm/530 nm yields the relation in Figure 8. This is one of the first examples of cure monitoring in photoinduced cationic cross-linking.

Conclusions

Fluorescent probe **1** is a sensitive molecular monitor for changes occurring in a cross-linking matrix before and after R_p^{max} for both radical and cationic systems. This is a benefit in comparison to intramolecular excimer probes, which work only above the glass transition temperature of the reacting material.[20] Classical charge-transfer probes cannot be used to probe cationic cross-linking because carbocations alkylate the tertiary amino function and may result in a loss of the charge-transfer properties in tertiary amino nitrogen bearing compounds such as 4-(dimethylamino)-4′-nitrostilbene,[2a] coumarins,[2a] (dimethylamino)naphthalenesulfonamides,[2b−d] or 1-phenyl-4-(4-cyano-1-naphthylmethylene)piperidine.[14] The new fluorescence probe introduced in this work can be applied to examine the photoinduced radical and cationic cross-linking process. A combination of fluorescence and other methods to measure conversion, i.e., FTIR or FT-Raman, allows construction of conversion−time profiles from fluorescence measurements.

Acknowledgment. The authors acknowledge the National Science Foundation (DMR-9526755) and the Office of Naval Research (ONR N00014-97-1-0834) for financial support of this work. Furthermore, the authors are pleased to thank Spectra Group, Ltd., for providing the cure monitor and the FTIR spectrometer.

References and Notes

(1) Contribution No. 386 from the Center for Photochemical Sciences.
(2) (a) Jager, W. F.; Volkers, A. A.; Neckers, D. C. *Macromolecules* **1995**, *28*, 8153. (b) Wang, Z. J.; Song, J. C.; Bao, R.; Neckers, D. C. *J. Polym. Sci., Part B: Polym. Phys.* **1996**, *34*, 325. (c) Hu, S.; Popielarz, R.; Neckers, D. C. *Macromolecules* **1998**, *31*, 4107. (d) Song, J. C.; Neckers, D. C. *Polym. Eng. Sci.* **1996**, *36*, 394.
(3) (a) Loutfy, R. O. *Pure Appl. Chem.* **1986**, *58*, 1239. (b) Loutfy, R. O. *J. Polym. Sci., Part B: Polym. Phys.* **1982**, *20*, 825. (c) Loutfy, R. O. *Macromolecules* **1981**, *14*, 270.
(4) (a) Strehmel, B.; Strehmel, V.; Timpe, H. J.; Urban, K. *Eur. Polym. J.* **1992**, *28*, 525. (b) Strehmel, B.; Strehmel, V.; Younes, M. *J. Polym. Sci., Part B: Polym. Phys.* **1999**, *37* 1367. (c) Younes, M.; Wartewig, S.; Lellinger, D.; Strehmel, B.; Strehmel, V. *Polymer* **1994**, *35*, 5269.
(5) (a) Levy, R. L.; Schwab, S. D. *Polym. Compos.* **1991**, *12*, 96. (b) Levy, R. L.; Schwab, S. D. *Polym. Mater. Sci. Eng.* **1988**, *59*, 596.
(6) Miller, K. E.; Burch, E. L.; Lewis, F. D.; Torkelson, J. M. *J. Polym. Sci., Part B: Polym. Phys.* **1994**, *32*, 2625.
(7) (a) Wang, F. W.; Lowry, R. E.; Grant, W. H. *Polymer* **1984**, *25*, 690. (b) Wang, F. W.; Bur, A. J.; Lowry, R. E.; Fanconi, B. M. *Polym. Mater. Sci. Eng.* **1988**, *59*, 600. (c) Lin, K.-F.; Wang, F. W. *Polymer* **1994**, *35*, 687.
(8) Hale, A. M. C. W.; Bair, H. E. *Macromolecules* **1991**, *24*, 2610, 1253.
(9) (a) Yu, W. v. M. E. D. *Macromolecules* **1990**, *23*, 882. (b) Nöel, C.; Laupretre, F.; Friedrich, C.; Leonard, C.; Halary, J. L.; Monnerie, L. *Macromolecules* **1986**, *19*, 201.
(10) Decker, C. *Polym. Int.* **1998**, *45*, 133.
(11) (a)Levy, R. L. *Polym. Mater. Sci. Eng.* **1984**, *50*, 124, 169. (b) Levy, R. L.; Ames, D. P. *Org. Coat. Appl. Polym. Sci. Proc.* **1983**, *48*, 116.
(12) Song, J. C.; Sung, C. S. P. *Macromolecules* **1993**, *26*, 4818.
(13) Rettig, W.; Chandross, E. A. *J. Am. Chem. Soc.* **1985**, *107*, 5617.

(14) Mes, G. F.; de Jong, B.; van Ramesdonk, H. J.; Verhoven, J.; Warman, J. M.; de Haas, M. P.; Hoorsman-van den Dool, L. E. W. *J. Am. Chem. Soc.* **1984**, *106*, 6524.

(15) The photochemistry occurring in these compounds can be described in general with the following scheme including two species, the CT and the LE, with their corresponding geometry in the ground and excited state (marked by the asterisk):

$$\mathrm{LE} \underset{\text{fluorescence}}{\overset{\text{absorption}}{\rightleftharpoons}} \mathrm{LE}^* \xrightarrow{k_{\mathrm{LE}\rightarrow\mathrm{CT}}} \mathrm{CT}^* \underset{\text{absorption}}{\overset{\text{fluorescence}}{\rightleftharpoons}} \mathrm{CT}$$

The formation of CT* by LE* is assigned by the rate constant $k_{\mathrm{LE}\rightarrow\mathrm{CT}}$. This quantity can be related to molecular mobility.

(16) Strehmel, B.; Rettig, W. *J. Biomed. Opt.* **1996**, *1*, 98. Strehmel, B.; Seifert, H.; Rettig, W. *J. Phys. Chem. B* **1997**, *101*, 2232.

(17) Strehmel, V.; Frank, C. W.; Strehmel, B. *J. Photochem. Photobiol. A* **1997**, *105*, 353.

(18) Victor, J. G.; Torkelson, J. M. *Macromolecules* **1987**, *20*, 2241.

(19) Görner, H.; Kuhn, J. In *Advances in Photochemistry*; Neckers, D. C., Volman, D. H., von Bünau, G., Eds.; John Wiley & Sons: New York, 1995; Vol. 19, p 1.

(20) (a) Pajot-Augy, E.; Bokobza, L.; Monnerie, L.; Castellan, A.; Bouas-Laurent, H.; Millet, C. *Polymer* **1983**, *24*, 117. (b) Pajot-Augy, E.; Bokobza, L.; Monnerie, L.; Castellan, A.; Bouas-Laurent, H. *Macromolecules* **1984**, *17*, 1490. (c) Bokobza, L.; Pajot, E.; Monnerie, L.; Bouas-Laurent, H.; Castellan, A. *Polymer* **1981**, *22*, 1309.

(21) Strehmel, B.; Sarker, A. M.; Malpert, J. H.; Strehmel, V.; Seifert, H.; Neckers, D. C. *J. Am. Chem. Soc.* **1999**, *131*, 1226.

(22) (a) Saltiel, J.; Sears, D. F.; Sun, Y.-P.; Choi, J.-O. *J. Am. Chem. Soc.* **1992**, *114*, 3607. (b) Saltiel, J.; Waller, A. S.; Dears, D. F. *J. Am. Chem. Soc.* **1993**, *115*, 2453.

(23) Sanyo, H.; Hirayama, F. *J. Phys. Chem.* **1983**, *87*, 83.

(24) Calculation of the molecular orbitals (MOPAC Package, PM3 Hamiltonian) showed that the electron is localized at the aromatic rings bearing the alkoxy groups in the HOMO-1 orbital. No electron distribution can be found in the fluorinated ring for that orbital. A reverse pattern was observed for consideration of the LUMO+1 showing electron distribution fully on the fluorinated ring and no electron distribution for the terminal aromatic rings. These changes of electron distribution draw the classical picture for intramolecular transfer, and one can include these patterns to discuss the probe properties as long as the HOMO-1 → LUMO-+1 configuration contributes mainly to the excited state.

(25) Suppan, P.; Ghoneim, N. *Solvatochromism*; Royal Society of Chemistry: Cambridge, England, 1997.

(26) A photostationary state consisting of both the cis and the trans isomer is formed during irradiation. Because both isomers can absorb radiation, an emission that resulted would arise of both isomers. A spectral decomposition is not possible in many cases.

(27) Reichardt, C. *Chem. Rev.* **1994**, *94*, 2319.

(28) Enhanced photochemistry for **1r** and **2r** was proved via H NMR experiments in CD_3CN. Irradiation of **1r** showed new peaks in the NMR spectrum, which were at 6.68 ppm (10 Hz doublet, cis-olefin) and at 5.05 and 4.79 ppm (cyclobutane). Illumination of **2r** gave a similar pattern with new peaks at 6.94 ppm (doublet, 10 Hz) and 5.47 ppm. The formation of cyclobutane structures results from 2 + 2 photocycloaddition. This occurs under the experimental conditions because the concentration of **1r**, as well as **2r**, is much higher (1 wt %) than it was in the fluorescence experiments (0.01 wt % during cure monitoring). We do not know whether 2 + 2 photocycloaddition occurs only at high concentration so we cannot exclude this reaction under dilute conditions.

(29) Probes that have the capability to probe the polarity of the molecular surrounding can give information about mobility changes as well. Because the relaxation time of dipoles change with temperature and viscosity, the probes respond to these changes.

(30) A calibration function for the setup described was obtained by approximation of the data in Figure 5b with a polynomial function.

MA990773B